

# BCS-BEC crossover of the strongly interacting ${}^6\text{Li}$ - ${}^{40}\text{K}$ mixture

Stefano Gandolfi,<sup>1</sup> Ryan Curry,<sup>2,1</sup> and Alexandros Gezerlis<sup>2</sup>

<sup>1</sup>*Theoretical Division, Los Alamos National Laboratory, Los Alamos, New Mexico 87545, USA*

<sup>2</sup>*Department of Physics, University of Guelph, Guelph, Ontario N1G 2W1, Canada*

We present Quantum Monte Carlo calculations of the properties of a two-component mass imbalanced Fermi gas, corresponding to the  ${}^6\text{Li}$ - ${}^{40}\text{K}$  mixture. We compute the equation of state of the unpolarized system as a function of the scattering length with particular attention paid to the unitary limit, where the effect of the effective range of the interaction is explored. We have also computed the pair distribution function and the momentum distribution over a range of interaction strengths to provide information about the structure of the system. Finally, we have computed the heavy/light quasiparticle spectrum. Our theoretical predictions, based on Quantum Monte Carlo calculations, can be tested by future experiments with ultracold fermionic gases.

## I. INTRODUCTION

In recent years much work has been addressed to study ultra-cold Fermi gases, both experimentally and theoretically (for a complete review see for example Ref. [1]). Through the use of a Feshbach resonance it is possible to tune the interaction between fermions as desired [2], and the amazing experimental control on these systems gives access to beautiful experiments where Fermi gases can be studied under a range of conditions. It is possible to probe the entire BCS-BEC crossover [3] where the system can be tuned from a BCS state where fermions are weakly interacting, to the unitary regime where the two-body scattering length is infinite, to a BEC condensate of Bosons. When the population imbalance changes, the system can eventually exhibit different phases [4, 5] where superfluid and normal phases may coexist or phase separate [6, 7], or other intriguing more exotic phases like the Larkin-Ovchinnikov-Fulde-Ferrell (LOFF) phase or  $p$ -wave superfluidity could appear [8, 9].

Considerable experimental effort has been spent on the investigation of trapped mass imbalanced two-component Fermi gases. Early work explored mainly systems consisting of a mixture between  ${}^6\text{Li}$  and  ${}^{40}\text{K}$  atoms [10–15], and in recent years experimental probes have been conducted for a wide variety of mass-imbalanced systems [16–22] with various mass ratios. There has also been continued interest in probes of the  ${}^6\text{Li}$  –  ${}^{40}\text{K}$  mixture, such as investigations into dimer stability [23].

The properties of the mass imbalanced system can be very different from the equal mass case; for example, with a majority light population the Chandrasekhar-Clogston limit is very small and close to zero [24]. Then, at unitarity, a two-component Fermi gas with unequal masses may exhibit very different properties with respect to the equal mass case [25, 26], even at the mean field level [27, 28]. Systems of mass imbalanced fermions also show new features in the few-body sector. The binding energy of an impurity has been calculated in Ref. [29]; however, finite systems with few-heavy atoms that interact with a single light one through a two-body potential with infinite scattering length have very intriguing non-universal properties [30–32], and this could effectively modify the

many-body structure of the state with polarization, supporting new phases that do not show in the equal mass case [28, 33–35]. It has also been shown that for very large mass ratios the ground state of the unpolarized system might be solid [36, 37]. In addition, there is rich physics to explore in mass imbalanced systems existing in lower dimensions, such as novel types of pairing [38] and quarteting [39].

Since experiments are possible at very low temperatures, of the order of fractions of  $T_F$ , the zero temperature effects can directly be compared to or extrapolated from experiments. Several  $T = 0$  predictions for equal mass Fermi gases were made in the past by means of Quantum Monte Carlo techniques (QMC)[24, 40–45], and later confirmed by experiments for both the equal [46] and unequal mass [47] cases. The Variational Monte Carlo (VMC) and the Diffusion Monte Carlo (DMC) methods allow one to accurately solve for the ground-state of strongly interacting many body systems, and have been widely used in the study of diverse physical systems such as condensed matter, quantum chemistry, nuclear physics, and cold atomic physics [48–54]. Previous studies have explored the properties of strongly interacting fermions at unitarity [55] however, the theoretical study of the unequal mass system has not received a similar effort as the equal mass case.

In this paper we focus on a Fermi-Fermi mixture with a mass ratio  $m_h/m_l=6.5$  corresponding to the  ${}^6\text{Li}$ - ${}^{40}\text{K}$  mixture, and we study the BCS-BEC crossover by employing QMC techniques; in particular in this work we compute properties of the unpolarized system with equal number of heavy and light atoms. We first compute the equation of state that is crucial to fit density functionals used to compute properties of trapped larger systems [56–58]. We compute the energy per particle as a function of the scattering length of the two-body interaction by paying particular attention to the effect of the finite effective range of the potential. We have also computed the pair distribution function between heavy and light particles as well as the momentum distribution. These quantities are useful to extract the contact parameter that can be measured in experiments, similar to the equal mass case [59, 60]. We then simulate the system with very small po-

larization in order to study the quasiparticle dispersion as a function of the interaction. These calculations serve to carefully explore the properties of  ${}^6\text{Li}$ - ${}^{40}\text{K}$  system and provide stringent theoretical predictions for future experiments.

## II. MODEL

We model our system by considering point-like interacting particles with the following Hamiltonian:

$$H = \frac{-\hbar^2}{2m_l} \sum_{i=1}^{N_l} \nabla_i^2 + \frac{-\hbar^2}{2m_h} \sum_{j'=1}^{N'_h} \nabla_{j'}^2 + \sum_{i,j'} v(r_{ij'}), \quad (1)$$

where  $N_l$  and  $N'_h$  is the number of particles with mass  $m_l$  and  $m_h$ , and  $v(r_{ij'})$  is a  $s$ -wave short-range interaction acting only between fermions of different species. The form of  $v(r)$  we use is the Pöschl-Teller already employed in several previous QMC calculations [24, 40–42, 55, 56, 58, 61]:

$$v(r) = -v_0 \frac{\hbar^2}{m_r} \frac{\mu^2}{\cosh^2(\mu r)}, \quad (2)$$

where  $m_r$  is the reduced mass, and the parameters  $\mu$  and  $v_0$  are tuned in order to reproduce the effective range  $r_e$  and the scattering length  $a$  of the interaction. For this potential, the unitary limit corresponding to the zero-energy ground-state between two particles is achieved with  $v_0 = 1$  and  $r_e = 2/\mu$ . We consider a system in the dilute limit, meaning that the interparticle distance  $r_0 \gg r_e$ , where  $r_0 = (9\pi/4)^{1/3}/k_F$  and  $k_F$  is the Fermi momentum of the system. Most of the results presented in this work were obtained by fixing  $r_e k_F \approx 0.03$  but in several cases we considered different values to check effects due to the effective range of the potential.

The ground-state of the system is solved by means of QMC techniques, i.e. the VMC and the DMC. The many-body wave function [40, 41], is given by,

$$\Psi_T = \left[ \prod_{ij} f(r_{ij'}) \right] \Phi_{\text{BCS}}. \quad (3)$$

The Jastrow function  $f(r)$  acts between particles with different masses, and it is obtained by solving the equation

$$-\frac{\hbar^2}{2m_r} \nabla^2 f(r) + v(r)f(r) = \lambda f(r). \quad (4)$$

The parameter  $\lambda$  is obtained by imposing the boundary condition  $f(r > d_0) = 1$ , where the healing distance  $d_0$  is a variational parameter. The correct boundary conditions to the wave function are guaranteed by constraining  $d_0 \leq L/2$  where  $L$  is the size of the simulation box, but we find that a typical good choice is  $d_0 \approx L/10$ . By solving

Eq. (4) we also assure the correct behavior of the wave function at small distances so that the Jastrow function  $f$  is defined to have  $\partial f/\partial r=0$  at the origin. This condition must be satisfied in order to have a finite kinetic energy in the origin when computing  $\nabla^2 f = f''(r) + 2f'(r)/r$ . This condition is necessary to avoid spurious contributions to the energy computed using QMC.

The antisymmetric part  $\Phi_{\text{BCS}}$  is a particle-projected BCS wave function including pairing correlations (see the appendix of Ref. [62]). It is given by

$$\Phi_{\text{BCS}} = \mathcal{A}[\phi(r_{11'})\phi(r_{22'})\dots\phi(r_{N_l N'_h})]. \quad (5)$$

The operator  $\mathcal{A}$  antisymmetrizes like particles, the unprimed coordinates are for light particles, the primed are for heavy particles, and  $N_l = N'_h = N/2$  for the unpolarized case. The pairing function is expressed as

$$\begin{aligned} \phi(\mathbf{r}) &= \beta(r) + \sum_n a(k_n^2) \exp[i\mathbf{k}_n \cdot \mathbf{r}], \\ \beta(r) &= \tilde{\beta}(r) + \tilde{\beta}(L-r) - 2\tilde{\beta}(L/2), \\ \tilde{\beta}(r) &= [1 + \gamma br] [1 - \exp(-dbr)] \frac{\exp(-br)}{dbr}. \end{aligned} \quad (6)$$

The function  $\beta(r)$  has a range of  $L/2$ , and the value of  $\gamma$  is chosen such that  $\beta(r)$  has zero slope at the origin. Note that if  $\beta(r) = 0$ , and  $a(k_n^2) = 0$  for  $|\mathbf{k}_n| > k_F$ ,  $\Phi_{\text{BCS}} = \Phi_{FG}$ , where the latter is a Slater determinant wave function describing the non-interacting Fermi gas in the normal phase. As  $\Phi_{FG}$  and  $\Phi_{\text{BCS}}$  are orthogonal, we can study the Fermi gases both in the superfluid and in the normal phase [6, 7]. The pairing wave function used here contains 12 free parameters that have been optimized by minimizing the energy of the system using VMC and following the strategy of Ref. [63]. In the case of strong interactions, when  $1/ak_F \geq 2$ , we found that using the pairing function as in Ref. [44], i.e. the two-body wave function instead of the function of Eq. (6), gives lower energies. Instead, in the BCS case for  $1/ak_F \leq -1$ , the BCS wave function  $\Phi_{BCS}$  gives almost the same energy of  $\Phi_{FG}$  as the pairing becomes less and less important.

Polarized systems can be simulated by extending the wave function to include single-particle states for the unpaired particles [40, 41]. Note that the wave function as previously described cannot reproduce more exotic phases like LOFF or  $p$ -wave pairing.

The ground-state of the system is then solved by projecting the wave function in imaginary time by means of the DMC technique (see for example Ref. [41]). It is important to note that the DMC algorithm strictly provides an upper-bound to the energy, and thus it is a variational calculation within the fixed-node approximation used to control the Fermion sign problem. However, if the global structure of the wave function is carefully optimized, the DMC provides a very accurate estimate of the ground-state. The accuracy of the DMC has been tested by comparing the results of the equal mass unitarity Fermi gas with the Auxiliary Field Quantum

Monte Carlo (AFQMC) [45]. For purely attractive interactions, in AFQMC the unpolarized system is solved exactly with no sign problem. The agreement between DMC and AFQMC is within 4-5% giving us the confidence that once the wave function is carefully optimized the upper-bound to the energy given by DMC is very close to the energy of the ground state. It is straightforward to extend the DMC to deal with systems with unequal masses or with polarization by modifying the wave function, and the systematic error given by the fixed-node approximation should provide the same accuracy as for the unpolarized case, if the trial wave function correctly describes the phase of the system. Note that for polarized systems or for unpolarized systems with unequal masses the AFQMC suffers from a severe sign-problem, and the constrained-path used to control it does not provide an upperbound to the energy as the fixed-node approximation does for DMC.

### III. BCS-BEC CROSSOVER

We simulate a system of 66 fermions, as this has been shown to provide a very accurate description of fermionic systems in the thermodynamic limit [55, 56, 64]. We choose this particular number because the results found using a BCS-like wave function can be directly compared to the system in the normal phase. In the  $\Phi_{FG}$  wave function the single particle orbitals are plane waves, and the energy of 33 free fermions is very close to the infinite limit.

We show in Fig. 1 the equation of state of the unpolarized  ${}^6\text{Li}$ - ${}^{40}\text{K}$  mixture as a function of  $1/ak_F$ . For negative values of  $a k_F$  the two-body interaction does not admit a two-body bound state, and for positive values the two-body binding energy per particle has been subtracted from the total energy of the system. The results are in units of the non-interacting Fermi gas,  $E_{FG} = 3E_F/5$  where  $E_F = \frac{\hbar^2}{4m_r} k_F^2$ . It is clear that on the BCS side the energy per particle approaches the limit of the non-interacting Fermi gas. While on the BEC side, the energy per particle quickly becomes comparable to the two-particle binding energy showing the formation of strongly bound molecules, and  $(E - E_2/2)/E_{FG}$  rapidly tends to zero. All the points have been computed by setting the effective range of interaction corresponding to  $\mu/k_F = 60$  and tuning  $v_0$  to have the desired scattering length (blue circles in Fig. 1). For many points we investigated the effect of a finite effective range and repeated the calculation using  $\mu/k_F = 24$  (green squares). We note that the results become independent of the effective range for  $1/|a k_F| \geq 1$ , as seen by the essentially constant energy in the deep BEC regime.

As discussed above for  $1/ak_F > 1$  we found that the best variational wave function is provided by assuming the pairing wave function is the two-body solution as in Ref. [44]. By analyzing the structure of the wave function we can conclude that for  $1/ak_F \geq 2$  the system made

of attractive fermions is very well modeled by a weakly repulsive Bose gas. In this regime, if we use the pairing wave function of Eq. (6) the energy of the system is higher, and we would likely need many more plane-waves to correctly describe the short-range behavior of the two-particle solution.

The energy of a repulsive Bose gas, where Bosons are made by two fermions with different mass, can be well approximated by a mean-field expansion [65], that for unequal masses is given by:

$$\frac{E/N - E_2/2}{E_{FG}} = \frac{10}{9\pi} a_{dd} k_F \frac{m_h m_l}{(m_h + m_l)^2} \times \left[ 1 + \frac{128}{15\sqrt{6}\pi^3} (a_{dd} k_F)^{3/2} + \dots \right], \quad (7)$$

where  $a_{dd}$  is the Boson-Boson scattering length, whose value is obtained by fitting to our QMC calculations. The results in the strongly interacting regime are shown in the right inset of Fig. 1 for the mass ratio considered. The fit has been made in the  $1/ak_F \geq 2$  region giving  $a_{dd}/a = 0.886(4)$  in a good agreement with the few-body analysis of Ref. [66, 67]. The agreement between the QMC results and the mean field expansion of Eq. (7) starts to fail for  $1/ak_F < 2$ , indicating that the system is no longer similar to a Bose gas, as also suggested by

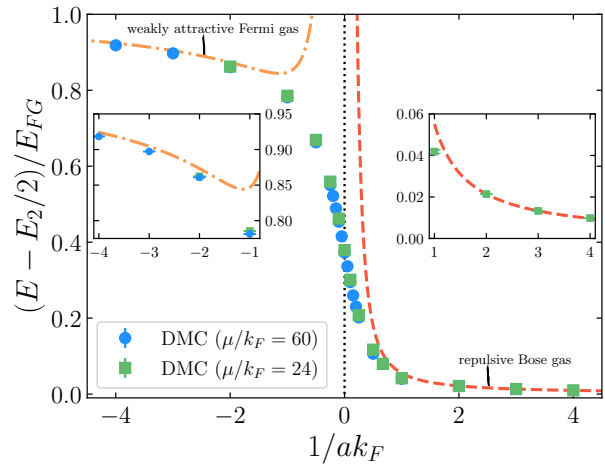


FIG. 1. (color online) The BCS-BEC crossover for the unpolarized  ${}^6\text{Li}$ - ${}^{40}\text{K}$  mixture as a function of  $1/ak_F$ . QMC results are shown for two potentials with different effective ranges (blue circles for  $\mu/k_F = 60$  and green squares for  $\mu/k_F = 24$ ). The energy is in units of the Fermi gas energy  $E_{FG}$  after the subtraction of the two-body binding energy per particle on the BEC side. The orange dashed line shows the perturbation expansion of a weakly attractive Fermi gas, and the red dashed line the equation of state of a repulsive Bose gas. In the left inset we show the energy per particle around unitarity with the fit given by Eq. (8). The right inset shows the comparison between QMC results and the equation of state of a repulsive Bose gas with a dimer-dimer scattering length  $a_{dd} = 0.886(4)a$ .

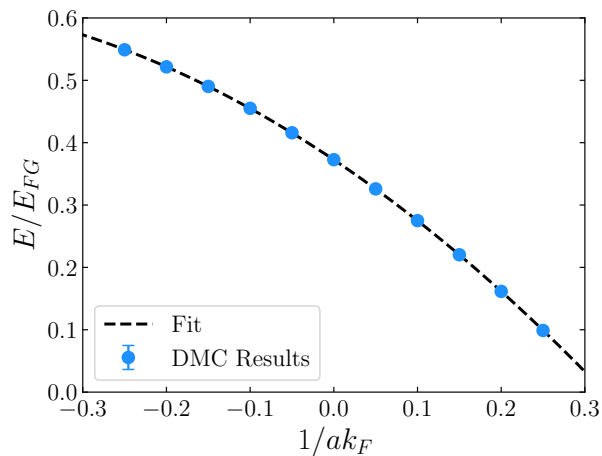


FIG. 2. (color online) The BCS-BEC crossover for the unpolarized  ${}^6\text{Li}$ - ${}^{40}\text{K}$  mixture as a function of  $1/ak_F$  near the unitary limit. Our results are compared against a fit given by Eq. (8) as discussed in the text.

looking at the structure of the many-body wave function.

In Fig. 2 we show the crossover around the unitary limit. Close to unitarity, the equation of state can be expanded as [59]

$$\frac{E}{E_{FG}} = \xi - \frac{\zeta}{k_F a} - \frac{5\nu}{3(k_F a)^2} + \dots \quad (8)$$

The fit to our QMC results gives  $\xi = 0.3726(6)$ ,  $\zeta = 0.900(2)$  and  $\nu = 0.46(1)$ . The values of  $\zeta$  and  $\nu$  are very similar to the case of equal masses reported in Ref. [55]. We also find a good qualitative agreement with the calculation of Ref. [68].

The various tests we performed indicate that around  $1/ak_F \approx 0$  the extrapolation to  $r_e \rightarrow 0$  just shifts the energy but does not change the curvature of the equation of state in the region where  $1/|ak_F| < 1$ . There, only the  $\xi$  parameter is particularly sensitive to  $r_e$  as is also the case for the equal mass system [55]. It is interesting to compare the finite range extrapolation to the unequal mass mixture to the equal mass case. The comparison is motivated for the  ${}^6\text{Li}$ - ${}^{40}\text{K}$  system as the resonance is more narrow than for equal masses [69] and consequently the unitary limit could be "less universal" and the effect of the effective range more important. We performed several calculations at unitarity for different values of  $r_e$  in order to test the finite range effects and extrapolated to zero effective range as shown in Fig. 3. The QMC points have been fit using the linear function

$$\frac{E}{E_{FG}} = \xi + cr_e k_F, \quad (9)$$

and the best estimate given by QMC is  $\xi = 0.368(1)$ . The value of  $c$  gives the slope of the extrapolation that is  $c = 0.13(1)$  for unequal masses. It is rather intriguing

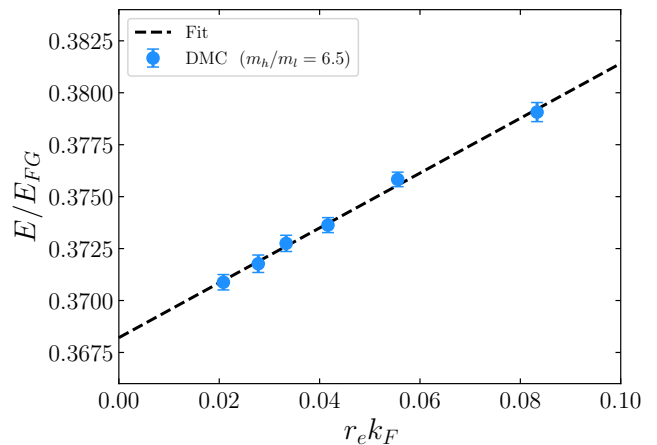


FIG. 3. (color online) The energy of the  ${}^6\text{Li}$ - ${}^{40}\text{K}$  mixture as a function of the effective range  $r_e$  of the interaction in the unitary limit. The energy is in units of the Fermi gas energy  $E_{FG}$ . The fit parameters are very similar to those found in the equal mass case in [55]. The details of the fit to the QMC results are discussed in the main text.

that the slope of the energy as a function of the effective range is very similar to the equal mass case [45].

We have also computed the pair distribution function  $g_{h-l}(r)$  between heavy and light particles, as shown in Fig. 4.  $g_{h-l}(r)$  is calculated by a mixed estimate of the form [71],

$$g_{h-l}(r) = \sum_{i < j'} \langle \Psi_0 | \delta(r_{ij} - r) O_{ij}^P | \Psi_T \rangle, \quad (10)$$

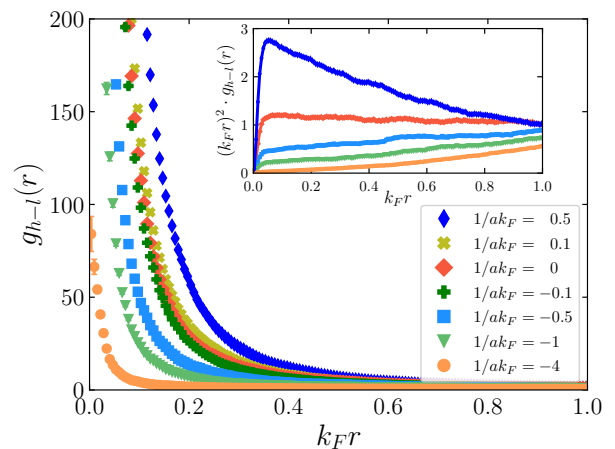


FIG. 4. (color online) Heavy-light pair distribution function for different two-body interactions indicated in the legend. From left to right they correspond to  $1/ak_F = -4, -1, -0.5, -0.1, 0, 0.1$  and  $0.5$ . In the inset we show the same function multiplied by  $(k_F r)^2$  for selected interaction strengths corresponding to  $1/ak_F = -4, -1, -0.5, 0$  and  $0.5$  (from the bottom to the top).



where  $\Psi_0$  is the DMC projected ground state.

The function  $g_{h-l}(r)$  exhibits a large peak at short distances, induced by the strong attractive interaction in the s-wave channel. In the weak coupling limit the value of the peak is smaller as expected, and is clear in the figure. In the inset of Fig. 4 we show  $(k_F r)^2 g_{h-l}(r)$  that can be used to extract the contact parameter as shown in Ref. [55]. The limit of  $(k_F r)^2 g_{h-l}(r)$  for short distances approaches zero in the BCS limit as the short-range correlations are weaker when the strength of the attractive interaction decreases. On the other side, in the strong coupling regime where  $1/ak_F = 0.5$ , the limit of  $(k_F r)^2 g_{h-l}(r)$  at small distances rapidly increases.

In Fig. 5 we show the momentum distribution of the mass imbalanced system, calculated as the Fourier transform of the one-body density matrix by,

$$n_{h-l}(k) = \frac{N_{h(l)}}{L^3} \int d\Omega d\delta r e^{i\mathbf{k}\cdot(\mathbf{r}'_n - \mathbf{r}_n)} \frac{\Psi_T(\mathbf{r}_1, \dots, \mathbf{r}'_n)}{\Psi_T(\mathbf{r}_1, \dots, \mathbf{r}_n)}, \quad (11)$$

where the integral over the solid angle is handled stochastically and the integral over  $\delta r = |\mathbf{r}'_n - \mathbf{r}_n|$  is carried out on a line to avoid statistical errors [71]. In the very weak coupling region with  $1/ak_F = -4$  the  $n(k)$  is very similar to the non interacting Fermi gas momentum distribution, where  $n(k) = 1$  for  $k < k_F$  and zero otherwise. Moving to strong couplings the tail of  $n(k)$  is longer, as expected, due to the strong pairing effects. This is well evident in the inset of Fig. 5 where the function  $(k/k_F)^4 n(k)$  is shown. The inset clearly shows the  $C/k^4$  universal behavior predicted by Tan [59, 60], where  $C$  is the contact parameter. For  $1/ak_F = 0$  the black dashed line shows the value of the contact derived from the equation of state [70] for Fig. 1 and Eq. (8).

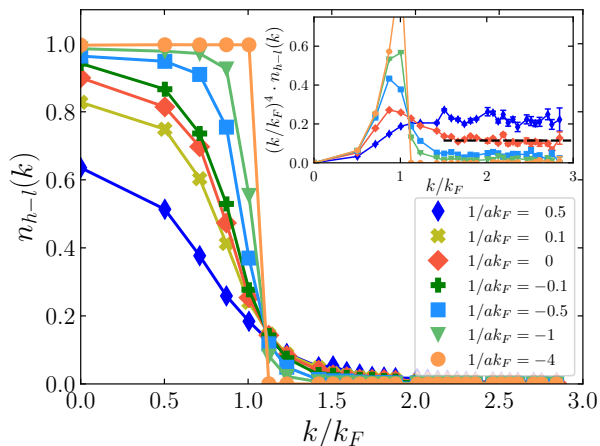


FIG. 5. (color online) Momentum distribution  $n(k)$  for different interaction strengths (same color convention as Fig. 4). In the inset we plot  $(k/k_F)^4 n(k)$  to show the tail behavior of the momentum distribution. The dashed black line shows the contact parameter  $C$  derived from the equation of state around the unitary limit [70].

#### IV. QUASIPARTICLE SPECTRUM

The quasiparticle dispersion is computed by adding an unpaired particle to the system [24, 40, 41, 71, 72]. We have carried out simulations of 67 particles where the unpaired particle is characterized by a finite momentum  $|k|$  and mass  $m_l$  or  $m_h$ . We then combine the result with the energy of the fully paired unpolarized system of 66 particles, and define the quasiparticle energy as

$$\epsilon(k)/E_F = [E_k(67) - E(66)]/E_F, \quad (12)$$

where  $k$  is the momentum of the extra particle, and  $E(67)$  and  $E(66)$  are the total energies of the systems with 67 and 66 particles. The two simulations have been performed at the same total density. In Ref. [24] the quasiparticle dispersion was computed by comparing the energy of the two systems at the same background density, then at constant volume. Here we have fixed the total density in order to avoid small effects due to the effective range of the interaction. However, the finite size effects should be very small as the volume of the simulation box is quite large.

The results of the quasiparticle dispersion in Fig. 6 show that the dispersion of light and heavy particles are very different from what has already been found at unitarity [24]. For each case the quasiparticle dispersion is lower on the BCS side and increases by crossing unitarity and moving to the BEC side. In particular for light quasiparticle the position of the minimum changes from about  $(k/k_F)^2 = 0.5$  at  $ak_F = -2$  to  $(k/k_F)^2 = 0$  at  $ak_F = 2$ .

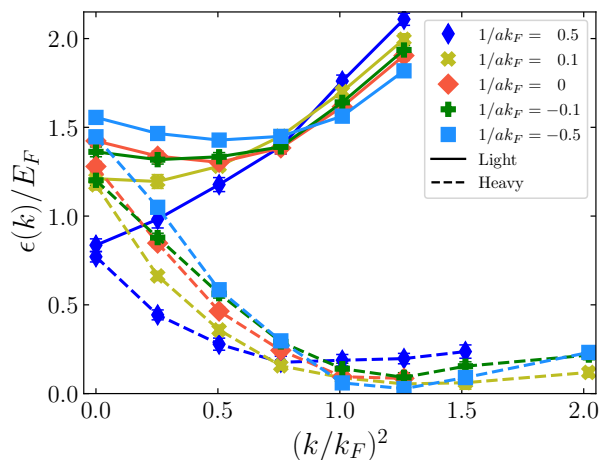


FIG. 6. (color online) Quasiparticle dispersion at different scattering lengths. The upper and lower curves show results for light (solid lines) and heavy (dashed lines) quasiparticles as a function of the momentum. We show results for the unitary limit (red diamonds) as well as the BCS region ( $ak_F < 0$ ) and the strong interacting BEC region ( $ak_F > 0$ ). All results correspond to a mass ratio  $m_h/m_l = 6.5$ .

## V. CONCLUSIONS

In this paper we show QMC results exploring the BCS-BEC crossover of the mass imbalanced  ${}^6\text{Li}$ - ${}^{40}\text{K}$  Fermi mixture. QMC techniques have been used in the past to give the best upperbound of the energy of strongly interacting fermions in the unitary limit. We made use of QMC to compute the equation of state as a function of the two-body scattering length, studying the crossover from the weakly interacting limit where the system is well described by the BCS theory, to the strong coupling limit where fermions form molecules, and the system is well described by a weakly repulsive Bose gas. We have carefully checked finite-range effects close to the unitary limit, and provided an accurate fit of the equation of state based on our QMC calculations. We also show other properties of the unpolarized superfluid system, namely the pair distribution function and the momentum distribution. Finally, by considering the system with very small polarizations, we have computed the heavy- and light-quasiparticle dispersion for different strengths of the interaction. These results should provide a comprehensive framework for future theoretical and experimental investigations into the

mass-imbalanced Fermi gas across the full range of the BCS-BEC crossover.

## ACKNOWLEDGMENTS

The work of S.G. is supported by the U.S. Department of Energy, Office of Nuclear Physics, under contract No. DE-AC52-06NA25396, and by the Office of Advanced Scientific Computing Research, Scientific Discovery through Advanced Computing (SciDAC) NUCLEI program. The work of R.C. and A.G. was supported by the Natural Sciences and Engineering Research Council (NSERC) of Canada and the Canada Foundation for Innovation (CFI). R.C. was also supported by the Laboratory Directed Research and Development program of Los Alamos National Laboratory under project number 20220541ECR. Computational resources have been provided by the Los Alamos National Laboratory Institutional Computing Program, which is supported by the U.S. Department of Energy National Nuclear Security Administration under Contract No. 89233218CNA000001. Computer time was also made available by the National Energy Research Scientific Computing Center (NERSC), and SHARCNET through the Digital Research Alliance of Canada.

- 
- [1] S. Giorgini, L. P. Pitaevskii, and S. Stringari, *Rev. Mod. Phys.* **80**, 1215 (2008).
- [2] C. Chin, R. Grimm, P. Julienne, and E. Tiesinga, *Rev. Mod. Phys.* **82**, 1225 (2010).
- [3] G. C. Strinati, P. Pieri, G. Röpke, P. Schuck, and M. Urban, *Physics Reports* **738**, 1 (2018).
- [4] M. W. Zwierlein, A. Schirotzek, C. H. Schunck, and W. Ketterle, *Science* **311**, 492 (2006).
- [5] G. B. Partridge, W. Li, R. I. Kamar, Y.-a. Liao, and R. G. Hulet, *Science* **311**, 503 (2006).
- [6] S. Pilati and S. Giorgini, *Phys. Rev. Lett.* **100**, 030401 (2008).
- [7] C. Lobo, A. Recati, S. Giorgini, and S. Stringari, *Phys. Rev. Lett.* **97**, 200403 (2006).
- [8] A. Bulgac, M. M. Forbes, and A. Schwenk, *Phys. Rev. Lett.* **97**, 020402 (2006).
- [9] A. Bulgac and M. M. Forbes, *Phys. Rev. Lett.* **101**, 215301 (2008).
- [10] E. Wille, F. M. Spiegelhalter, G. Kerner, D. Naik, A. Trenkwalder, G. Hendl, F. Schreck, R. Grimm, T. G. Tiecke, J. T. M. Walraven, S. J. J. M. F. Kokkelmans, E. Tiesinga, and P. S. Julienne, *Phys. Rev. Lett.* **100**, 053201 (2008).
- [11] M. Taglieber, A.-C. Voigt, T. Aoki, T. W. Hänsch, and K. Dieckmann, *Phys. Rev. Lett.* **100**, 010401 (2008).
- [12] F. M. Spiegelhalter, A. Trenkwalder, D. Naik, G. Kerner, E. Wille, G. Hendl, F. Schreck, and R. Grimm, *Phys. Rev. A* **81**, 043637 (2010).
- [13] T. G. Tiecke, M. R. Goosen, A. Ludewig, S. D. Gensemer, S. Kraft, S. J. J. M. F. Kokkelmans, and J. T. M. Walraven, *Phys. Rev. Lett.* **104**, 053202 (2010).
- [14] A.-C. Voigt, M. Taglieber, L. Costa, T. Aoki, W. Wieser, T. W. Hänsch, and K. Dieckmann, *Phys. Rev. Lett.* **102**, 020405 (2009).
- [15] A. Trenkwalder, C. Kohstall, M. Zaccanti, D. Naik, A. I. Sidorov, F. Schreck, and R. Grimm, *Phys. Rev. Lett.* **106**, 115304 (2011).
- [16] A. Khramov, A. Hansen, W. Dowd, R. J. Roy, C. Makrides, A. Petrov, S. Kotochigova, and S. Gupta, *Phys. Rev. Lett.* **112**, 033201 (2014).
- [17] C. Ravensbergen, V. Corre, E. Soave, M. Kreyer, E. Kirilov, and R. Grimm, *Phys. Rev. A* **98**, 063624 (2018).
- [18] C. Ravensbergen, E. Soave, V. Corre, M. Kreyer, B. Huang, E. Kirilov, and R. Grimm, *Phys. Rev. Lett.* **124**, 203402 (2020).
- [19] E. Neri, A. Ciamei, C. Simonelli, I. Goti, M. Inguscio, A. Trenkwalder, and M. Zaccanti, *Phys. Rev. A* **101**, 063602 (2020).
- [20] A. Ciamei, S. Finelli, A. Cosco, M. Inguscio, A. Trenkwalder, and M. Zaccanti, *Phys. Rev. A* **106**, 053318 (2022).
- [21] A. Green, H. Li, J. H. See Toh, X. Tang, K. C. McCormick, M. Li, E. Tiesinga, S. Kotochigova, and S. Gupta, *Phys. Rev. X* **10**, 031037 (2020).
- [22] F. Schäfer, Y. Haruna, and Y. Takahashi, *J. Phys. Soc. Jpn.* **92**, 054301 (2023).
- [23] M. Jag, M. Cetina, R. S. Lous, R. Grimm, J. Levinsen, and D. S. Petrov, *Phys. Rev. A* **94**, 062706 (2016).
- [24] A. Gezerlis, S. Gandolfi, K. E. Schmidt, and J. Carlson, *Phys. Rev. Lett.* **103**, 060403 (2009).
- [25] K. B. Gubbels, J. E. Baarsma, and H. T. C. Stoof, *Phys. Rev. Lett.* **103**, 195301 (2009).
- [26] J. E. Baarsma, K. B. Gubbels, and H. T. C. Stoof, *Phys. Rev. A* **82**, 013624 (2010).
- [27] M. A. Baranov, C. Lobo, and G. V. Shlyapnikov, *Phys. Rev. A* **78**, 033620 (2008).

- [28] J. Wang, Y. Che, L. Zhang, and Q. Chen, *Sci Rep* **7**, 39783 (2017).
- [29] R. Combescot, A. Recati, C. Lobo, and F. Chevy, *Phys. Rev. Lett.* **98**, 180402 (2007).
- [30] D. Blume and K. M. Daily, *Phys. Rev. A* **82**, 063612 (2010).
- [31] D. Blume and K. M. Daily, *Phys. Rev. Lett.* **105**, 170403 (2010).
- [32] Y. Castin, C. Mora, and L. Pricoupenko, *Phys. Rev. Lett.* **105**, 223201 (2010).
- [33] J. Braun, J. E. Drut, T. Jahn, M. Pospiech, and D. Roscher, *Phys. Rev. A* **89**, 053613 (2014).
- [34] D. Roscher, J. Braun, and J. E. Drut, *Phys. Rev. A* **91**, 053611 (2015).
- [35] M. Pini, P. Pieri, R. Grimm, and G. C. Strinati, *Phys. Rev. A* **103**, 023314 (2021).
- [36] D. S. Petrov, G. E. Astrakharchik, D. J. Papoular, C. Salomon, and G. V. Shlyapnikov, *Phys. Rev. Lett.* **99**, 130407 (2007).
- [37] O. N. Osychenko, G. E. Astrakharchik, F. Mazzanti, and J. Boronat, *Phys. Rev. A* **85**, 063604 (2012).
- [38] L. Rammelmüller, J. E. Drut, and J. Braun, *SciPost Physics* **9**, 014 (2020).
- [39] R. Liu, W. Wang, and X. Cui, *Phys. Rev. Lett.* **131**, 193401 (2023).
- [40] J. Carlson, S.-Y. Chang, V. R. Pandharipande, and K. E. Schmidt, *Phys. Rev. Lett.* **91**, 050401 (2003).
- [41] S. Y. Chang, V. R. Pandharipande, J. Carlson, and K. E. Schmidt, *Phys. Rev. A* **70**, 043602 (2004).
- [42] J. Carlson and S. Reddy, *Phys. Rev. Lett.* **95**, 060401 (2005).
- [43] J. Carlson and S. Reddy, *Phys. Rev. Lett.* **100**, 150403 (2008).
- [44] G. E. Astrakharchik, J. Boronat, J. Casulleras, and a. S. Giorgini, *Phys. Rev. Lett.* **93**, 200404 (2004).
- [45] J. Carlson, S. Gandolfi, K. E. Schmidt, and S. Zhang, *Phys. Rev. A* **84**, 061602 (2011).
- [46] M. J. H. Ku, A. T. Sommer, L. W. Cheuk, and M. W. Zwierlein, *Science* **335**, 563 (2012).
- [47] C. Kohstall, M. Zaccanti, M. Jag, A. Trenkwalder, P. Massignan, G. M. Bruun, F. Schreck, and R. Grimm, *Nature* **485**, 615 (2012).
- [48] D. M. Ceperley, *Reviews of Modern Physics* **67**, 279 (1996).
- [49] W. Foulkes, L. Mitas, R. Needs, and G. Rajagopal, *Reviews of Modern Physics* **73** (2001), 10.1103/RevModPhys.73.33.
- [50] J. Kolorenc̆ and L. Mitas, *Rep. Prog. Phys.* **74**, 026502 (2011).
- [51] A. Roggero, A. Mukherjee, and F. Pederiva, *Phys. Rev. B* **88**, 115138 (2013).
- [52] J. Carlson, S. Gandolfi, F. Pederiva, S. C. Pieper, K. Schmidt, and R. Wiringa, *Reviews of Modern Physics* **87** (2015), 10.1103/RevModPhys.87.1067.
- [53] L. M. Schonenberg and G. J. Conduit, *Phys. Rev. A* **95**, 013633 (2017).
- [54] S. Gandolfi, J. Carlson, A. Roggero, J. E. Lynn, and S. Reddy, *Physics Letters B* **785**, 232 (2018).
- [55] S. Gandolfi, K. E. Schmidt, and J. Carlson, *Phys. Rev. A* **83**, 041601 (2011).
- [56] M. M. Forbes, S. Gandolfi, and A. Gezerlis, *Phys. Rev. Lett.* **106**, 235303 (2011).
- [57] I. Bausmerth, A. Recati, and S. Stringari, *Phys. Rev. A* **79**, 043622 (2009).
- [58] M. M. Forbes, S. Gandolfi, and A. Gezerlis, *Phys. Rev. A* **86**, 053603 (2012).
- [59] S. Tan, *Annals of Physics* **323**, 2971 (2008).
- [60] S. Tan, *Annals of Physics* **323**, 2987 (2008).
- [61] A. J. Morris, P. López Ríos, and R. J. Needs, *Phys. Rev. A* **81**, 033619 (2010).
- [62] S. Gandolfi, A. Yu. Illarionov, F. Pederiva, K. E. Schmidt, and S. Fantoni, *Phys. Rev. C* **80**, 045802 (2009).
- [63] S. Sorella, *Phys. Rev. B* **64**, 024512 (2001).
- [64] G. Palkanoglou, F. K. Diakonou, and A. Gezerlis, *Phys. Rev. C* **102**, 064324 (2020).
- [65] T. D. Lee, K. Huang, and C. N. Yang, *Phys. Rev.* **106**, 1135 (1957).
- [66] D. S. Petrov, C. Salomon, and G. V. Shlyapnikov, *J. Phys. B: At. Mol. Opt. Phys.* **38**, S645 (2005).
- [67] J. Levinsen and D. S. Petrov, *Eur. Phys. J. D* **65**, 67 (2011).
- [68] R. B. Diener and M. Randeria, *Phys. Rev. A* **81**, 033608 (2010).
- [69] D. Naik, A. Trenkwalder, C. Kohstall, F. M. Spiegelhalder, M. Zaccanti, G. Hendl, F. Schreck, R. Grimm, T. M. Hanna, and P. S. Julienne, *Eur. Phys. J. D* **65**, 55 (2011).
- [70] F. Werner and Y. Castin, *Phys. Rev. A* **86**, 013626 (2012).
- [71] A. Gezerlis and J. Carlson, *Phys. Rev. C* **81**, 025803 (2010).
- [72] S. Gandolfi, A. Yu. Illarionov, S. Fantoni, F. Pederiva, and K. E. Schmidt, *Phys. Rev. Lett.* **101**, 132501 (2008).